ISSN 1512-1461

UDC: 538.9 Condensed matter Physics, Solid state Physics, Theoretical Condensed matter Physics

ANNEALING TIME DEPENDENCE OF STRUCTURAL AND OPTICAL PROPERTIES OF SPIN COATED CdS FILMS

D. M. C. U. Dissanayake and P. Samarasekara

Department of Physics, University of Peradeniya, Peradeniya, Sri Lanka

Abstract:
Effect of annealing time period on the structure of CdS films synthesized using spin coating was studied. Single phase of CdS could be crystallized in thin film form in the selected range of annealing time period. Texture coefficient was calculated to determine preferred crystal orientations. In addition, the degree of preferred orientation was calculated at different annealing time periods. Crystalline size, strain, dislocation density and lattice parameters were calculated using XRD patterns. Crystalline size gradually increases with the annealing time period. However, the strain and dislocation density gradually decrease with annealing time period. Optical band gap was determined using UV-visible spectroscopy. Optical band gap gradually decreases with the annealing time period due to the increases of crystalline size.
Keywords: *Spin coating, XRD patterns, optical band gap, particle size, texture coefficient*

1. Introduction:

CdS is a II-IV type semiconductor with a high band gap around 2.42 eV. Owing to the high band gap, CdS films are employed as a window material in CdS/CdTe solar cells. CdS is a n-type semiconductor with yellowish color. CdS is a potential candidate in the applications of light emitting diodes, sensors, photoconductors, optical mass memories and solar selective coatings. Nanostructures have attracted a great interest in recent years because of their unique chemical, physical, optical, electrical and transport properties. Owing to the high surface area, all nanostructured materials posses a high surface energy and thus, are thermodynamically unstable or metastable. CdS nanoparticles are considered to be a prime candidate in the applications in future opto-electronic devices, nanodevices and biological labeling due to availability of discrete energy levels, tunable band gap, size dependent chemical and physical properties, easy preparation techniques and better chemical stability.

Fabrication techniques of CdS thin films include spray pyrolysis [1], chemical bath deposition [2, 7,], electro deposition [3], screen printing [4], physical vapor deposition, vacuum evaporation [5], electron beam evaporation [6] and sol-gel spin coating. Among many deposition methods, sol-gel spin coating technique is extensively applied as a matrix material method to produce nanocomposites because it gives a higher specific surface area, superior homogeneity and purity, better microstructural control of metallic particles, narrow pore size and uniform particle distribution. The main advantages of the sol-gel method are its simplicity, low cost and its ability to obtain uniform films with good adherence and reproducibility in a relatively shorter processing time at lower sintering temperatures. Influence of sol aging time and annealing temperature on nanocrystalline CdS thin films has been investigated [8]. Previously, structural and optical characterization of sol-gel spin- coated nanocrystalline CdS thin film have been investigated [9].

Previously we have prepared film samples using chemical vapor deposition [10] and sputtering techniques [11, 12, 13] incorporated with expensive vacuum machines. However, spin coating technique was found to be low cost compared to above methods. CdS possesses some magnetic properties [14]. The Heisenberg Hamiltonian was used to describe the magnetic properties

ISSN 1512-1461

of ferromagnetic and ferrite films by us previously [15, 16, 17, 18, 19]. Previously band gap of semiconductor particles doped with salts have been investigated by measuring electrical properties [20]. In this manuscript, the variation of optical and structural properties of CdS films with annealing time period will be described

2. Experimental:

Initially two solutions have been prepared as following. Polyethylene Glycol (PEG) was dissolved in ethanol (CH_3CH_2OH), and acetic acid (CH_3COOH) was added to ethanoic solution under stirring which was continued for 1 hour. Cadmium nitrate ($Cd(NO_3)_2$) and thiourea ($CS[NH_2]_2$) were dissolved in ethanol under stirring which was continued for 1 hour. Two solutions were mixed and stirred again for 4 hours to obtain the final sols for deposition of thin films. CdS thin films were deposited on ultrasonically cleaned amorphous glass substrates by sol-gel spin-coating technique. Solution was applied onto the glass substrates at speeds of 1500, 2200 and 2400 rpm for 30 seconds. Thereafter, the samples were dried on a hot plate at 120 ^{0}C for 1 hour, and annealed at 300, 350, 400, 450 and 500 ^{0}C at five different annealing times of 20, 40, 60, 80 and 100 min in air. This method was repeated to fabricate multi layers of CdS films. CdS films with 10 layers were deposited.

Structural properties of film samples were determined using X ray diffraction (XRD) with Cu-Kα radiation of wavelength 1.54060 Å. UV-visible spectrometer Shimadzu UV1800 was employed to investigate the optical properties of samples.

3. Results and discussion:

All the samples described in this section were spin coated at spin speed of 2200 rpm for 30 s. Figure 1 shows XRD patterns of CdS films with 10 layers annealed at 350 ^{0}C for 40, 60 and 80 minutes. According to XRD patterns, polycrystalline films with single phase of CdS could be synthesized in this range of annealing time period. The diffraction peaks observed for all films at angular positions of 24.9^0, 26.6^0, 28.2^0, 43.7^0, 47.7^{0}and 51.7^0 are corresponding to (100), (002), (101), (110), (103) and (112) reflections of CdS thin films, respectively, as confirmed by ICDD-PDF file 772306. With increasing annealing time, an additional peak starts to emerge at 36.6^0 corresponding to (102) reflection. Further, films ensure hexagonal wurtzite structure at this temperature since phase transformation from cubic to hexagonal occurs around 240-300 ^{0}C.

XRD patterns show that the peak intensity gradually increases with the annealing time. This can be assign to the growth of material and improvement of crystallinity of films upon annealing. The angular positions of reflections are found to shift slightly towards higher values due to increase of lattice constants. Following table 1 and figure 2 show the texture coefficients of CdS thin films and its variation with respect to annealing time.

ISSN 1512-1461

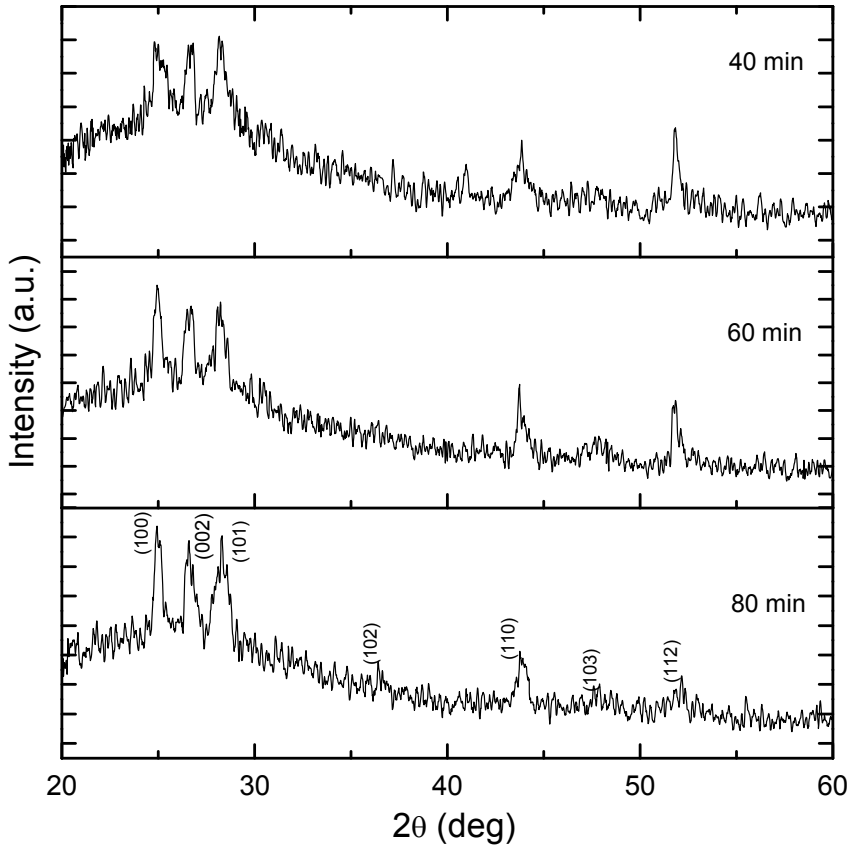

Figure 1: XRD patterns of CdS thin films with 10 layers annealed for different time periods at 350 ^{0}C.

Texture Coefficient	C_{100}	C_{002}	C_{101}	C_{110}	C_{103}	C_{112}
40 min	0.03	0.07	0.06	0.08	5.59	0.07
60 min	0.14	2.86	0.16	0.01	3.04	0.01
80 min	0.12	0.11	0.18	0.03	5.43	0.03

Table 1: Texture coefficients of CdS thin films annealed at different time periods

The texture coefficient (C_{hkl}) of a certain crystal plane (hkl) in a polycrystalline thin film is given as following.

$$C_{hkl} = \frac{\mathrm{I(hkl)/I_0(hkl)}}{(1/\mathrm{N})[\Sigma_{\mathrm{N}}\mathrm{I(hkl)/I_0(hkl)}]} \quad (1)$$

ISSN 1512-1461

Where, h,k,l = Miller indices corresponding to the diffraction peak

I(hkl) = Measured intensity

I_0(hkl) = JCPDS standard intensity of the corresponding powder

N = Number of reflections

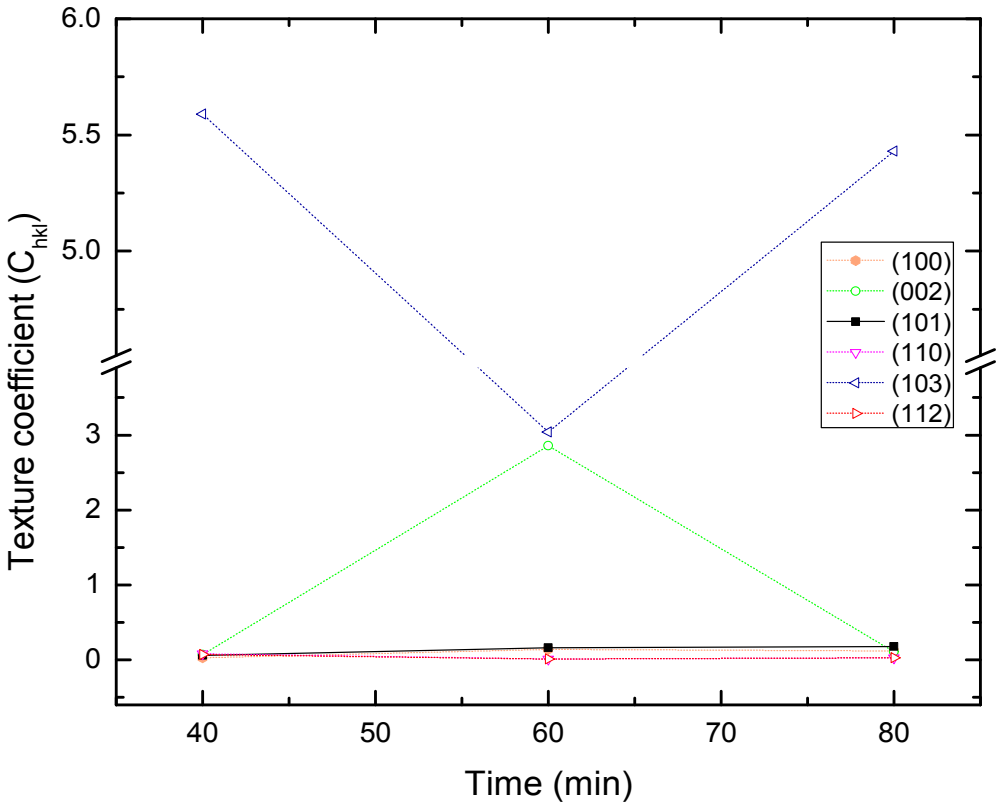

Figure 2: Variation of C_{hkl} of CdS thin films with annealing time

Quantitative evidence related to the preferential crystal orientation is given by the texture coefficient. According to above figure, texture coefficient of (101) plane increases as annealing time is increased indicating the more (101) preferred orientation of spin coated CdS thin films. The degree of preferred orientation (σ) calculated for thin films with different annealing times are presented in following table 2. The value of σ can be calculated as following.

$$\sigma = \sqrt{\frac{\sum_{i=1}^{N}(C_{hkl} - C_{0hkl})^2}{N}} \qquad (2)$$

Where, σ = Degree of preferred orientation

C_{0hkl} = Texture coefficient of powder sample which is always unity

ISSN 1512-1461

Time (min)	σ
40	2.05
60	1.38
80	1.98

Table 2: Variation of degree of preferred orientation of CdS thin films with annealing time

A value of zero for σ indicates that the sample is completely at random orientation. Above table shows that σ drops to a minimum at 60 min from the highest value at 40 min. Then, again σ starts to increase with annealing time. This indicates that the annealing time also can affects the degree of preferred orientation of thin films same as well as the annealing temperature. The interplanar spacing varies in the range of 3.161-3.157 Å as annealing time is increased. These values were calculated using the most intense (101) plane with standard value of 3.161 Å and thereby obtained results are in agreement with the given standard value.

Annealing Time (min)	D (nm)	a (Å)	c (Å)	ε (x 10^{-4})	δ(10^{14} lines/m^2)
40	7.383	4.099	6.693	47.514	183.48
60	12.892	4.119	6.726	27.208	60.165
80	14.732	4.126	6.737	23.810	46.076

Table 3: Crystalline size (D), lattice parameters (a and c), strain (ε) and dislocation density (δ) of CdS thin films annealed for different time periods at 350 ^{0}C

Similarly, the crystalline size, lattice parameters (a and c), strain and dislocation density were evaluated using (101) reflection of thin films with respect to annealing time. These values are tabulated in table 3.

The crystallite size (D) of the films is estimated using the Debye-Scherrer formula [8].
$D = \frac{0.91\lambda}{\beta \cos\theta}$, where λ is the X –ray wavelength (CuK_α = 1.54060 Å), β is the full width at half maximum (FWHM) of the dominant peak and θ is the Bragg angle.

The dislocation density (δ) and strain (ε) of CdS nanostructures were determined using these XRD results and following relations, respectively. $\delta = \frac{1}{D^2}$ and $\varepsilon = \frac{\beta \cos\theta}{4}$.
In addition, the lattice parameters *a* and *c* were calculated by following relations, respectively. $a = \frac{\lambda}{\sqrt{3}\sin\theta}$ and $c = \frac{\lambda}{\sin\theta}$.

The crystallite size (D) of the films is estimated using the Debye-Scherrer formula [8].

ISSN 1512-1461

$D = \frac{0.91\lambda}{\beta \cos\theta}$, where λ is the X –ray wavelength (CuK$_\alpha$ = 1.54060 Å), β is the full width at half maximum (FWHM) of the dominant peak and θ is the Bragg angle.

The dislocation density (δ) and strain (ε) of CdS nanostructures were determined using these XRD results and following relations, respectively. $\delta = \frac{1}{D^2}$ and $\varepsilon = \frac{\beta \cos\theta}{4}$.
In addition, the lattice parameters *a* and *c* were calculated by following relations, respectively.
$a = \frac{\lambda}{\sqrt{3}\sin\theta}$ and $c = \frac{\lambda}{\sin\theta}$.

Figure 3 is the graphical representation of the variation of crystalline sizes and strain as a function of annealing time. The crystalline sizes of CdS particles increase from 7.383 nm to 14.732 nm as the annealing time increases from 40 to 80 min. This behavior can be explained by the coarsening of the tiny crystals with high reactivity that is stimulated at long annealing durations. These activated sites then starts to grow consuming thermal energy that they acquire from annealing and finally creates larger grains. The longer the annealing duration, acquisition of thermal energy is larger and therefore the grain growing is larger with increase of annealing time.

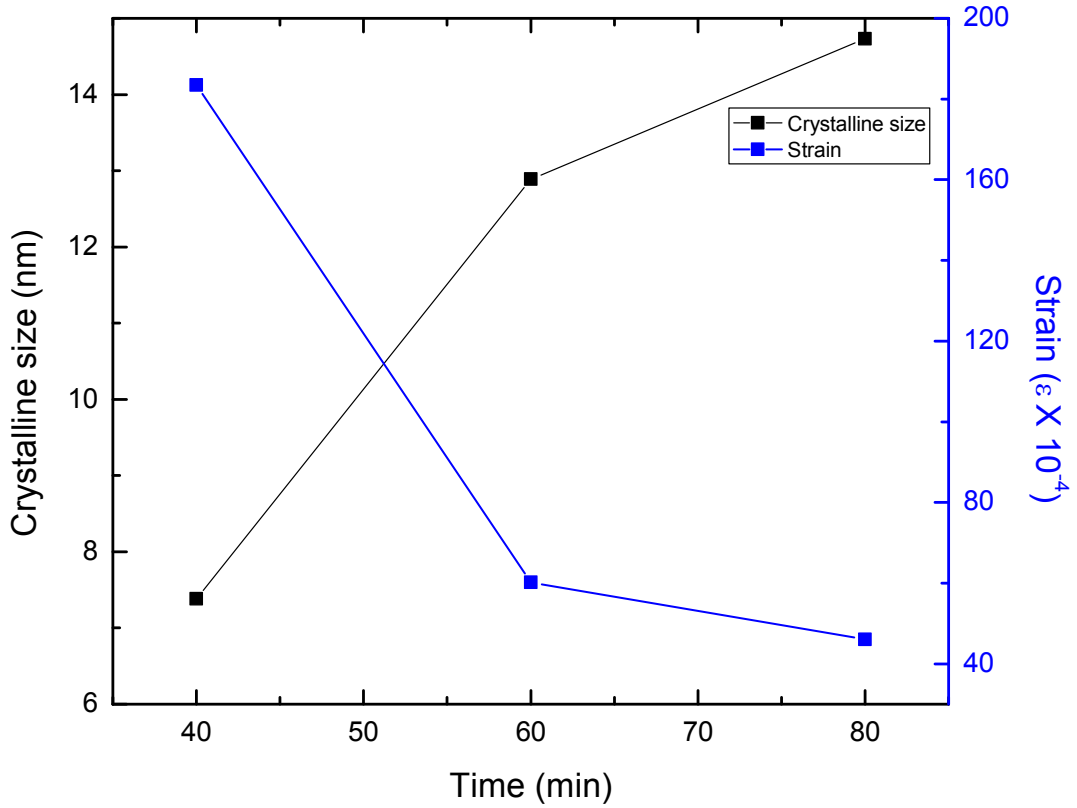

Figure 3: Variation of crystalline sizes and strain of CdS thin films with respect to annealing time

The lattice strain found to be decreasing with annealing time and it represents in the same figure. After annealing, films evolve to a state of compression as compared to the normal lattice state and will reduce the tensile strain. With excess of thermal energy gained from longer period of annealing,

ISSN 1512-1461

more and more number of atoms will rearrange to relive the tensile stress. Therefore, strain decreases with annealing time. The variation in strain is proportional to the amount of lattice defects. To be exact, the reduction of strain triggers a reduction in the concentration of lattice imperfections with the annealing time. The calculated values of lattice parameters, a, is less than that of the standard sample of ICDD-PDF file 772306 (a_{std}=4.136Å) whereas c value is greater (c_{std}=6.713 Å). Furthermore, these values increase with annealing time. This may be attributing to extrinsic stress caused by thermal mismatch.

Figure 4 shows absorbance of CdS films with 10 layers annealed at 350 ^{0}C for 20, 40, 60, 80 and 100 minutes. UV absorption decreases yet again with increasing wavelength. Spectra shows a sharp edge around 500 nm and films annealed for 100 min shows a much shaper edge. At this point, absorption of UV radiation decreases with decrease of annealing time. Further, the absorption edge shifts towards longer wavelengths with increasing annealing time.

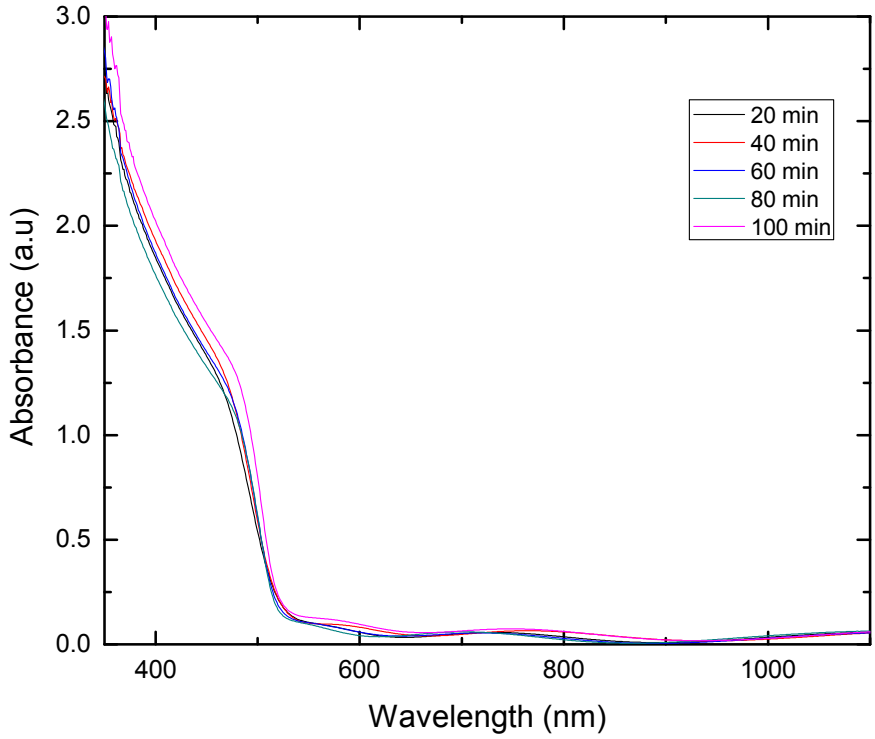

Figure 4: Absorption spectra of thin films annealed at 350 ^{0}C for (a) 20 min, (b) 40 min, (c) 60 min, (d) 80 min and (e) 100 min with 10 layers

Transmittance spectrum of thin films annealed for different time periods is shown in Figure 5. All films exhibit a high transparency (around 90%) at longer wave length region and a sudden fall near the absorption edge around 500 nm.

ISSN 1512-1461

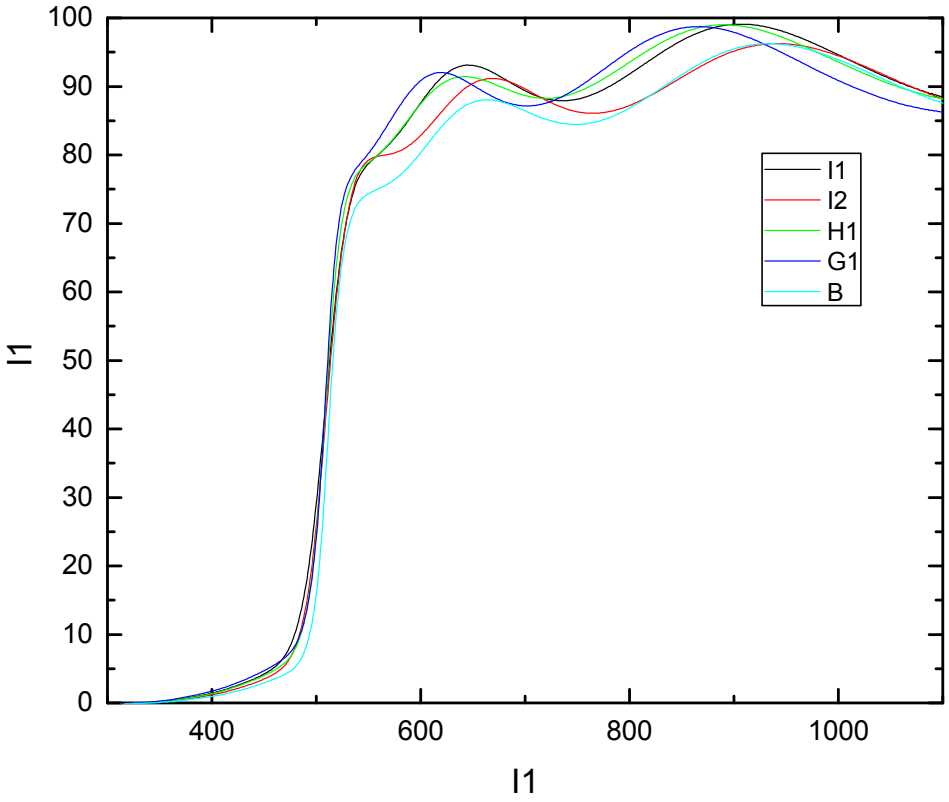

Figure 5: Transmittance spectra of thin films annealed at 350 ^{0}C for (a) 20 min, (b) 40 min, (c) 60 min, (d) 80 min and (e) 100 min with 10 layers

In general, optical transmittance decreases with annealing time. Annealing of thin films will evaporate water from the film surface. At longer annealing time periods the amount of water evaporates increases resulting surface roughness and thermally induce defects. Therefore, optical transmission decreases with annealing time due to the same reason as transmission decreases with annealing temperature. Interference fringes appear in the spectrum at longer wave lengths indicates the formation of homogeneous thin films.

Band gap values estimated using absorption spectra for different annealing times are given in table 4. It is clear that the increment of annealing time tends to reduce the optical band gap energy. Optical bang gap shows a tendency of decreasing with annealing time as shown in Figure 6. Annealing for longer period of time will provide more energy to atoms to diffuse in the lattice and produce saturated bonds. Thereupon, defects will be reduced and the crystallinity and stress relaxes will improve. As a result, density of localized states will decrease triggering band gap to be decrease with increasing annealing time.

Time (min)	Band gap (eV)
20	2.450
40	2.446
60	2.438
80	2.433
100	2.422

Table 4: Variation of optical band gap values with annealing time

ISSN 1512-1461

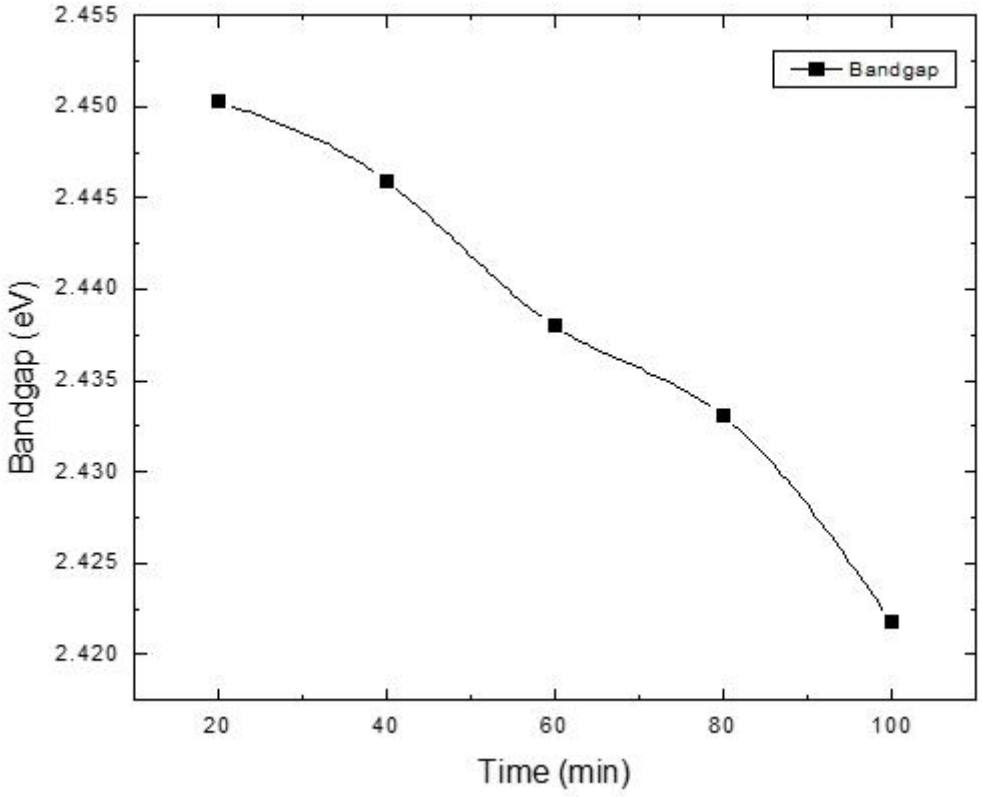

Figure 6: Optical band gap variation with annealing time

4. Conclusion:

All the thin film samples are consist of single phase of CdS, and found to be polycrystalline. Texture coefficient of (101) plane gradually increases with annealing time period. Texture coefficients of (100) and (002) plane first increase and then decrease with annealing time period.
Crystalline size increases from 7.383 to 14.732 nm as the annealing time period is increased from 40 to 80 min. However, strain decreases from 47.514×10^{-4} to 23.810×10^{-4}, and dislocation density decreases from 183.48×10^{14} to 46.076×10^{14} lines/m^2 as the annealing time period is increased from 40 to 80 min. Both the strain and dislocation density are related to the defects. When the sample is annealed for a longer time period, the crystallization improves and the number of defects reduces. As a result, both the strain and dislocation density decrease with annealing time period. Optical band gap gradually decreases from 2.450 to 2.422 as the annealing time period is increased from 20 to 100 min. The optical band gap decreases with the increase of crystalline size. This phenomenon can be explained using the Brus equation.

ISSN 1512-1461

References:

1. A.A. Yadav, M.A. Barote and E.U. Masumdar, Solid sate sciences (2010), 12(7), 1173.
2. P. Lisco, P.M. Kaminski, A. Abbas, K. Bass, J.W. Bowers, G. Claudio, M. Losurdo and J.M. Walls, Thin solid films (2015), 582, 323.
3. M. Takahashi, S. Hasegawa, M. Watanabe, T. Miyuki, S. Ikeda and K. Iida, Journal of applied electrochemistry (2002), 32, 359.
4. V. Kumar, D.K. Sharma, M.K. Bansal, D.K. Dwivedi and T.P. Sharma, Science of sintering (2011), 43(3), 335.
5. 1. K. Yilmaz, Journal of Ovonic Research (2014), 10(6), 211.
6. Yang Dingyu, Zhu Xinghua, Wei Zhaorong, Yang Weiqing, Li Lezhong, Yang Jun, and Gao Xiuying, Journal of Semiconductors (2011), 32(2), 023001 1-4.
7. Be Xuan Hop, Ha Van Trinh, Khuc Quang Dat, Phung Quoc Bao, VNU journal of science, mathematics –Physics (2008), 24, 119.
8. I. Rathinamala, J. Pandiarajan, N. Jeyakumaran and N. Prithivikumaran, International Journal of Thin Films science and Technology (2014), 3(3), 113.
9. M.A. Olopade, A.M. Awobode, O.E. Awe and T.I. Imalerio, International journal of research and reviews in applied sciences (2013), 15(1), 120.
10. P. Samarasekara, Chinese Journal of Physics (2009), 47(3), 361.
11. P. Samarasekara, Georgian Electronic Scientific Journals: Physics (2010), 2(4), 3.
12. P. Samarasekara and N.U.S. Yapa, Sri Lankan Journal of Physics (2007), 8, 21.
13. P. Samarasekara, A.G.K. Nisantha and A.S. Disanayake, Chinese Journal of Physics (2002), 40(2), 196.
14. X.G. Zhao, J.H. Chu and Z. Tang, The journal of physical chemistry (2015), 119(52), 29075.
15. P. Samarasekara and Udara Saparamadu, Georgian electronic scientific journals: Physics (2012), 1(7), 15.
16. P. Samarasekara and N.H.P.M. Gunawardhane, Georgian electronic scientific journals: Physics (2011), 2(6), 62.
17. P. Samarasekara, Electronic Journal of Theoretical Physics (2008), 5(17), 227.
18. P. Samarasekara and Udara Saparamadu, Research & Reviews: Journal of Physics-STM journals (2013), 2(2), 12.
19. P. Samarasekara and Udara Saparamadu, Georgian electronic scientific journals: Physics (2013), 1(9), 10.
20. K. Tennakone, S.W.M.S. Wickramanayake, P. Samarasekara and, C.A.N. Fernando, Physica Status Solidi (a) **(**1987) 104, K57.

Article received: 2020-01-28